



Novel Amorphous Carbon Thin Film (ACTF) from Rice Straw to Remove Sodium Ions from Synthetic Saline Water

Mahmoud Fathy*, Mahmoud Ahmed Mousa, TH Abdel Moghny, Abdel-Hameed AA El-Bellihi and Ahmed E Awadallah

Egyptian Petroleum Research Institute (EPRI), Cairo, Egypt

Abstract

Rice straw fibers, considered in this work are a good source for synthesized amorphous carbon thin film (ACTF) hence; it has 64% cellulose linen fibers. We study the structure and properties of ACTF as new adsorbents to study the individual adsorption characteristics of sodium ions from synthetic water. Batch tests, used to study the influence of pH, contact time, and temperature, on the ion adsorption on activated carbon. We found that the pseudo-second-order kinetic model and by Langmuir isotherm would portray contact time of sodium adsorption and isothermal adsorption steadies, respectively. Also the adsorption process of sodium ions on activated carbon is stronger depends on pH. The maximum adsorption capacities of sodium on activated carbon were 107, 120 and 135 mg g⁻¹ at 35, 45, and 65°C. The thermodynamic parameters explain that the adsorption of sodium ions on novel ACTF was a spontaneous process and endothermic reaction. According to adsorption studies, activated carbon suitable for ion chromatography or desalinate sodium ion in ion exchange process in the hybrid desalination process with insignificant loss of adsorption capacity. However, the ACTF has better properties than any other carbon materials that got from an agricultural by-product.

Keywords: Sodium ions; Activated carbon; Adsorption isotherm; Amorphous carbon; Cellulose; Rice straw; Chromatography

Introduction

The annually renewable agricultural residues represent an abundant, inexpensive, and available source of renewable lingo-cellulosic biomass, and their utilizations are attracting increased interest around the world, particularly for the production of novel materials for environmentally friendly industrial utilizations after chemical modification. Surface adjustments of initiating carbon have been connected as of late to upgrade the scattering property and adsorption limits of carbon materials, particularly amorphous carbon [1,2]. Amino, carboxyl, and hydroxyl functionalities assume a noteworthy part in developing complex structures in a blend with other utilitarian gatherings or the first structure of the carbon materials.

As is known, the major component making seawater saline is NaCl. Very wise chlorine is about 16 times higher than Mg, ~ 22 times than sulfur, ~ 48 times than Br and K. Similarly sodium is 9 times higher than Mg, 12 times to sulfur, 17 times to K and 180 times higher than Br and C [3,4]. Although NaCl is primarily present in much higher proportions, seawater does not merely consist of sodium chloride. If we want to remove only NaCl from water, it would still be unfit for drinking [5,6].

The process of desalination is based on heat based distillation as this or reverse osmosis (RO is now more common because the costs per unit of volume are lower in the long term.) There are different methods to remove sodium ions like reverse osmosis that changing seawater to freshwater. Hence, the reverse osmosis filter is used. With this reverse osmosis filter, all the mineral elements, as well as the impurities contained in seawater, are removed, making this close to pure freshwater [7]. Adsorption, i.e., Separation of sodium chloride from water, is the simple process for removal of NaCl from seawater [8]. Unlike desalination, the energy requirement in adsorption process is very small, and it can even work under gravity. The advent of Nano science and technology manifested by nonmaterial's including such nanostructures that possess ACTF new carbon materials having pores and surface structures will lead to the exploration of nonmaterial for adsorption process [9]. Recently, instead of pores embedded in polymer

membrane, the native pores of carbon nanostructures, particularly ACTF, will have caught attention for absorption of sodium from the water [10].

Hybrid configurations encompass straightforward structures with a low degree of coupling between membrane and ion exchange processes but range up to very complex configurations with strong interconnections on both the water side and adsorption or ion exchange process, as well as with several desalination processes connected in series or in parallel [11-13].

Likewise picking up in significance are worried about ecological contamination and maintainable advancement while selecting seawater desalination and force plant setups, and additionally their improvement while considering desalination and electricity overall [14]. In the useful configuration of hybrid thin film membrane and ion exchange systems, viewpoints become known, however, that confine is connecting of the two frameworks and joint usage of offices, as imagined in studies and reasonable outline examinations [15,16].

The discoveries of the designing of this plant and the thought that, by expanding interconnection between the two procedures on the water side, it is conceivable to propel a half-breed arrangement of this sort as to cost streamlining in the layer establishment. By joint usage of the admission hardware, viewpoints result for connected examination endeavors over the close and long terms, for instance: long haul conduct of films at lifted temperatures, propensity for biofouling in layer procedure with regular use of cooling water and saline solution, impacts of such interconnections on the general accessibility of the

***Corresponding author:** Dr. Mahmoud Fathy, Egyptian Petroleum Research Institute (EPRI), 1 Ahmed El-Zomer, Nasr City, Box No 11727, Cairo, Egypt, Tel: +20222747847; Fax: +20222747433; E-mail: fathy8753@yahoo.com (or dr.abo_fathy@yahoo.com)

Received April 04, 2016; Accepted June 20, 2016; Published June 30, 2016

Citation: Fathy M, Mousa MA, Moghny THA, El-Bellihi AAA, Awadallah AE (2016) Novel Amorphous Carbon Thin Film (ACTF) from Rice Straw to Remove Sodium Ions from Synthetic Saline Water. Adv Recycling Waste Manag 1: 111. DOI: 10.4172/2475-7675.1000111

Copyright: © 2016 Fathy M, et al. This is an open-access article distributed under the terms of the Creative Commons Attribution License, which permits unrestricted use, distribution, and reproduction in any medium, provided the original author and source are credited.

facility. Be that as it may, likewise for the operation and support association of such extensive offices, the outcomes can be predicted for the future advancement of half-breed plants [17], especially for operation administration and association of the interaction of the diverse force plant and desalination hybrid system, observing of SWRO layer substitution and cleaning, and additionally controlling water quality [18].

The goals of this feature of exploration were to assess the adsorption conduct of sodium ions on amorphous carbon thin film produced from rice straw waste and their functioning as far as adsorption limit and liking. To accomplish these objectives, the impact of trial climate, such as contact time, pH scale and temperature, on the adsorption process of sodium ions were analyzed. The adsorption thermodynamics and energy forms on amorphous carbon thin film were also considered. The operational simplicity, precision, What's more, the precision of the suggested ACTF recommend that it might be a chance to be a great elective for that determination from claiming inorganic cations On water Furthermore offer different requisitions Likewise desalination Also ion chromatography identification.

Materials and Methods

Materials and reagents

Analytical-grade sulfuric acid (Aldrich-Egypt), silica gel (Aldrich-Egypt), couplet nitrate (Aldrich- Egypt) and sodium chloride standards (Baker, Serbia), Rice straw from Egyptian company, NaOH (Aldrich-Egypt).

Characterization of adsorbent

Scanning electron microscopy (SEM) (Carl Zeiss, Germany). The (TEM) analysis was done using jouel2000 electron microscope at 200 kV. Data of X-ray diffraction (XRD) were obtained by (Bruker AXS, Germany) (Cu $k_{\alpha 1}$ radiation, $\lambda=1.54059 \text{ \AA}$). Studying Raman and Fourier-transform infrared (FTIR) spectra mode evaluated using a BOMEM (Hartmann & Braun) spectrometer in the transmission. KBr disk used to study the FTIR spectra of the samples.

Preparation of the couplet silicate nanoparticles

The couplet nanoparticles were coated with uniform silica layers according to Ref. [19] Method. In this respect, 4.0 g of the freshly prepared couplet silicate was vigorously stirred with 200 mL of ethanol for 30 min at 45°C, and then 40 mL water, and 4 mL (1.4 M) NaOH was added to the above suspension. Then the powder was separated and being too dry at 50°C for eight h in a vacuum oven to obtain couplet silicate nanoparticles.

Rice straw pretreatments

pretreatment process needed for rice straw. Cellulose solubilized by the dilute acid hydrolysis at 120°C for 60 min, using 1% (wt/wt) sulphuric acid, to face the delignification process at 120°C for 60 min using sodium hydroxide (1M). During the dilute acid hydrolysis, delignification process removed lignin and silica present in the pretreated rice straw into the black liquor.

Chemical exfoliation of cellulose

Five grams of cellulose were added to 5 mL concentrated sulfuric acid in the presence of 0.1 g silica and steered for 10 min., Then filtrated and washing with hot water till pH 7 and saving in oven at 40°C for 6 hours. The prepared cellulose was poured in a flask in the presence of 0.01 g cobalt silicate nanoparticles and heated up to 40°C for 30 min. The prepared carbon nanomaterial's left to cool for 1 hour, and then dried in a vacuum oven for 24 hours at 50-70°C.

Adsorption experiments

10 mL sodium ions solution added to 1 mg of activated carbon thin film with certain pH to study the adsorption investigations. solution bottles placed in a water bath, that was operated at certain temperatures and 2 hours [20]. An ultrasonic bath used to maintain the temperature. A 0.4 μm microfiltration membrane filter used to filter the aqueous samples and the concentrations of sodium ions infiltrate determined using atomic absorption spectroscopy (AAS) [21].

Effect of pH

To measure the effect of pH on Na^+ absorption, the solutions pH values between 2.1 and 12.0 prepared using buffered using concentration of HCL and NaOH solutions at 35°C. The ideal pH esteem dictated similarly as seven to Na^+ , what's more, utilized all around every one of adsorption experiment [22].

Kinetic and isothermal study

The effect of contact time on adsorption of Na^+ ions on ACTF studded in time range about 5-120 minute. To perform adsorption isotherm experiments we use different initial sodium concentrations of (C_0). The concentrations of stock sodium solutions ranged between 50 and 500 mg L^{-1} . We study the thermodynamic adsorption experiments at 35, 45, and 65°C. The difference between the initial concentration and the equilibrium concentration used to determine the amount of adsorbed Na^+ [23,24].

Results and Discussion

Amorphous carbon thin film characterization

FTIR analysis: FTIR analysis determines the different functional groups (carboxyl's, lactones, ketone, and phenols) on the surfaces of Amorphous Carbon Thin Film. From the noncrystalline, amorphous carbon spectrum Figure 1, we found a band at 3659 cm^{-1} indicating the presence of the OH functional group, and a band at 1100 cm^{-1} indicating the presence of the C=O stretching beyond. carbon shape in all stereochemistry has always formed poor marks in the infrared unless it's chemically treated with oxidation [25]. The FTIR spectra of amorphous carbon resin in Figure 1 exhibited the characteristic bands at 697, 1449 and 1491 cm^{-1} represent the mono-substituted aromatic ring of amorphous carbon. The bending vibration band of the polystyrene rings in the plane and appears at 1027 cm^{-1} [26]. Also Figure 1 has shown the fairly broad band at about 3460 cm^{-1} that assigned to the bending vibration of the OH group, which was probably caused by the drifting of its stretching, vibration toward the low frequency direction, under the hydrogen bond interaction between the H_2O molecule and the oxygen atom of the amorphous carbon [27].

Raman analysis: Raman spectra of amorphous carbon thin films (ACTF) are given in Figure 2. The Raman spectrum of the ACTF displays broadened prominent G peak at 1592 cm^{-1} that shifted corresponding to the first-order scattering of the E_g mode from 1582 cm^{-1} [2,28]. The D band at 1363 cm^{-1} becomes sheltered, shows the reduction in the size of the in-plane sp^2 domains, because the extensive oxidation process. This feature of change suggests a decrease in the average size of the sp^3 upon oxidation of the exfoliated graphite nanoparticles and the value of $I/I_0=0.333$ indicate the highly succeed in the preparation of TACTF with a high degree of crystallinity and low defecates.

SEM analysis: Morphological image of amorphous carbon thin film synthesized from rice straw studied by SEM and is shown in Figure 3. The external surface showed the best porous structure in chemically activated carbon by Co silicates and acid reagent as this surface was

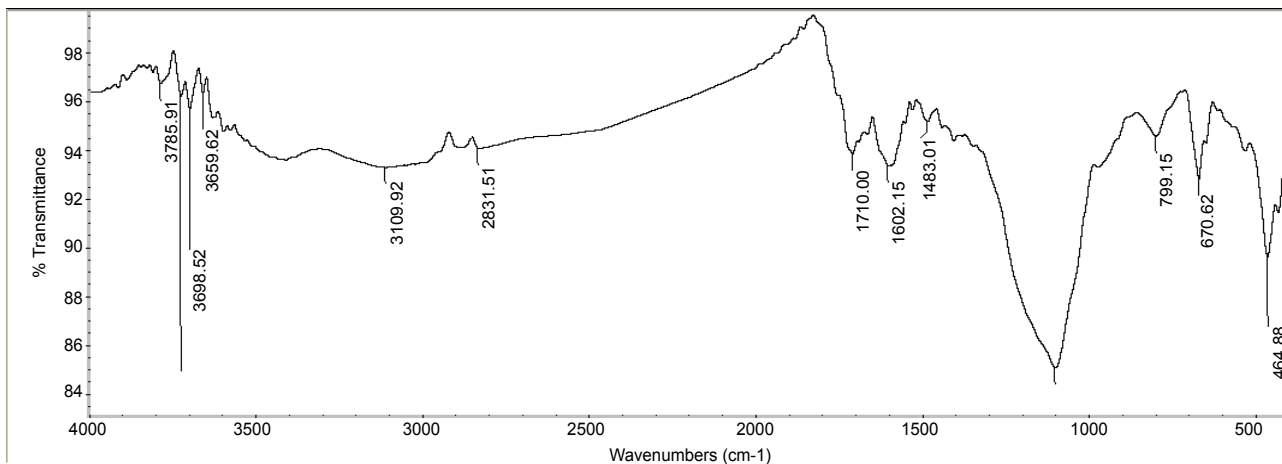


Figure 1: FTIR of amorphous carbon thin film from rice straw.

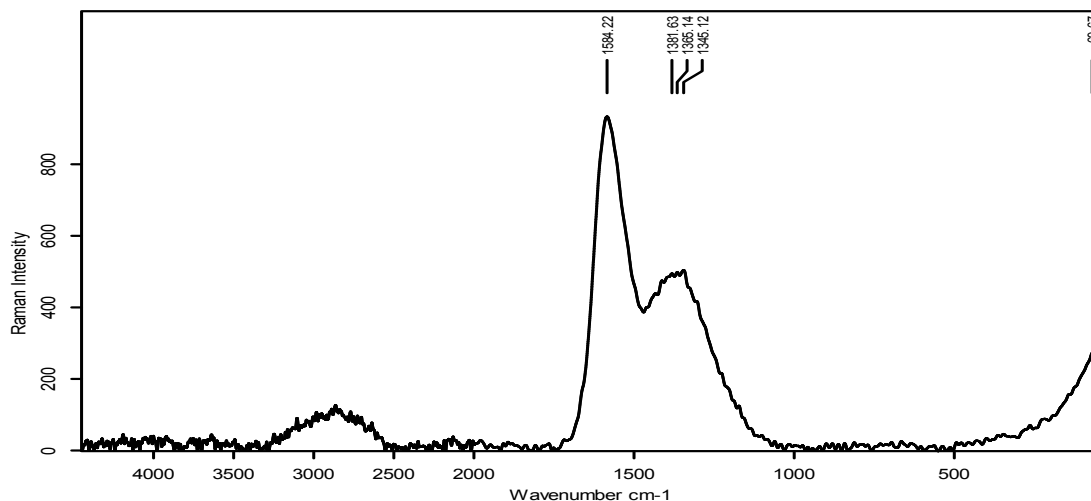


Figure 2: Raman analysis of amorphous carbon thin film from rice straw.

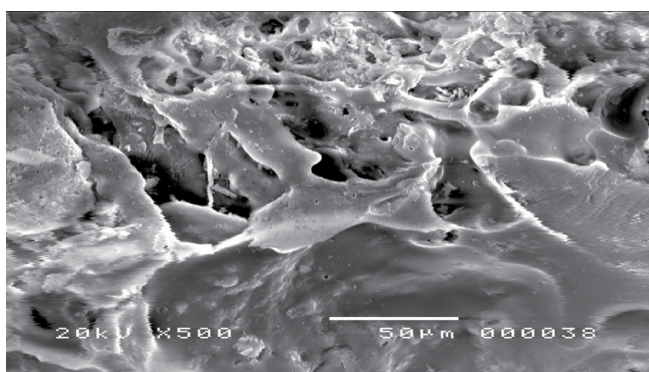


Figure 3: SEM of amorphous carbon thin film from rice straw.

rich in pores, comparing with other literature the surface of the carbon activated physically had no porous structure except for some occasional cracks [29]. We found that the acidic groups that found on the surface of ACTF could give numerous adsorption sites and thereby increase ACTF adsorption capacities for Na^+ ions. In addition, the morphology

image illustrated that the ACTF adhere to each other, therefore, the interspaces between ACTF is significantly reduced. Based on our recent SEM analysis, there is the presence of inter-particle repulsions forces between carboxylic groups on the surface of ACTF in smaller-sized “globs” of ACTF that result in smaller ACTF aggregates of carboxyl-functionalized ACTF. This feature of result shows that it possible to use, the functioned ACTF as adsorbents in the treatment of polluted water and sewer water.

TEM analysis: TEM used to study the morphology of ACTF and the structure of carbon materials surface, and pictures are appearing in Figure 4. After oxidation and amination TEM pictures of ACTF delegate that the surface of ACTF is not smooth, clean, and there is undeniable change, at first, glance structure. The commonplace width of ACTF was assessed to be in the scope of 40–100 nm. The ACTF materials fundamentally comprise of sheets because of auxiliary imperfections, which are relied upon to give dynamic destinations to adsorption. Likewise, vicinity of utilitarian gatherings at the surface of ACTF fundamentally affects their adsorption properties.

Effect of pH: Figure 5 shows the effect of pH on adsorption of Na^+ on ACTF. We found that the pH of arrangement assumes is an

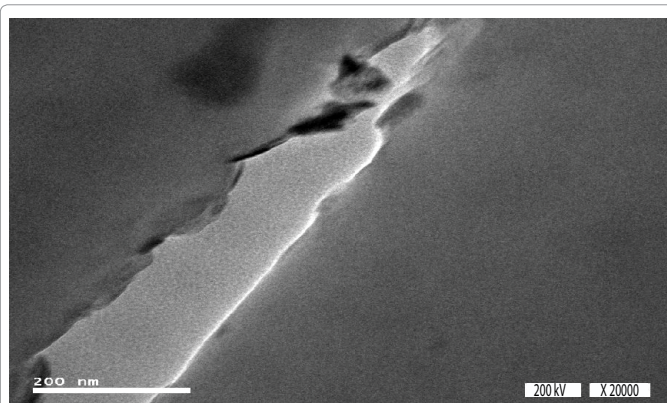


Figure 4: High-Resolution TEM of transparent amorphous carbon thin films.

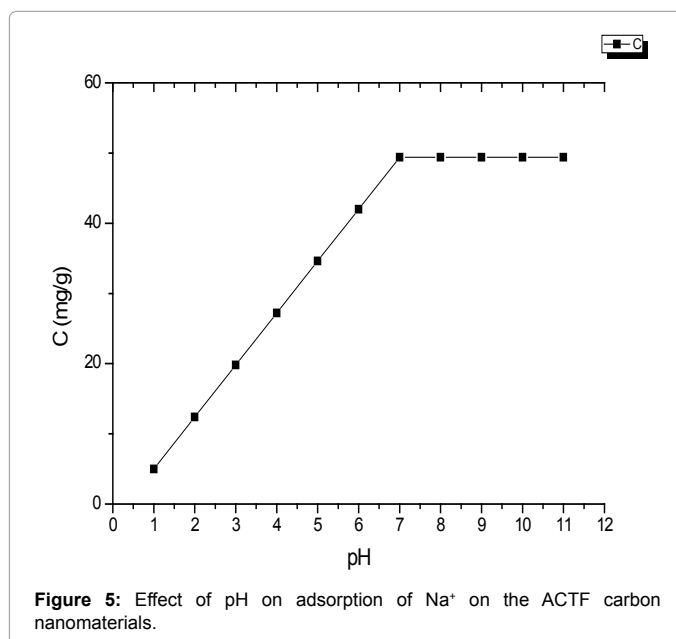


Figure 5: Effect of pH on adsorption of Na⁺ on the ACTF carbon nanomaterials.

imperative part on Na⁺ absorption attributes on ACTF. The evacuation of Na⁺ concentration was rapidly at pH 2–7, and gradually in the pH score of 7–11. Harmony centralizations of Na⁺ ionic species, at diverse pH, are a useful premise for the discourse of the adsorption mechanism [30,31]. the absorption of sodium ions become fixed when the ph more than 7 because the saturation at active site on the ACTF that Specific subtracted experimentally from all available amount of sodium ions, so these is the reliable values of absorbed sodium we obtained. Figure 5 shows the significant dependence of Na⁺ absorption on ACTF and, at different pH. The competition between H⁺ and Na⁺ lead to low Na⁺ absorption at low pH. We concluded that pH higher than 3 is beneficial for the ionization of the acidic surface groups, such as carboxylic groups and others groups (pK_a 3–6), that play a significant role in the uptake of Na⁺ ions.

Kinetic studies

Contact time study of the removal of sodium ions from aqueous solution by ACTF at pH 7 as showed that the process faster at first 60 min for adsorption of Na⁺ on ACTF and that was sufficient to achieve the adsorption equilibrium illustrated in Figure 6.

Analyzing the regression coefficients (R²) values of the parameters for the pseudo-first and pseudo-second-order rate adsorption kinetic

models were utilized in this feature of study the adsorption of sodium ions on ACTF. We found that the parameters of pseudo-second-order are the best fitted to explain the data of contact time study. The separation of the variables of the pseudo-second-order in the differential form and integration are given in (Equation 1),

$$\frac{t}{q_t} = \frac{1}{K' q_e^2} + \left(\frac{1}{q_e}\right)t \quad [32] \quad (1),$$

where q_e and q_t are the amounts of metal ion adsorbed (mg g⁻¹) at equilibrium and at time t , respectively. K' [g mg⁻¹ min⁻¹] is the pseudo-second-order rate constant of adsorption [33-35].

Plotting t/q_t against T gives values of q_e , K , and R^2 (Table 1). The q_e values (Table 1) viewing the good agreement with the results of testing work. The special form in the church of pseudo-second-order kinetics, which is common for that taken away of metals ions by carbonaceous materials, gives a sign of that the concentrations of both support Na⁺ and adsorbent (ACTF) are needed in the rate coming to a decision about the step of the adsorption process. In addition, we indicate that the slower absorption rates on ACTF indicate that the adsorption of sodium ions having a higher energetic barrier. It may be such as conception and/or surface complexation, are working.

Adsorption isotherms study

To describe adsorption characteristics of ACTF two adsorption idealized models have been used, namely, the Langmuir Eq. [2,36,37] and Freundlich (Equation 3), in their linearized forms:

$$q_e = \frac{b q_{\max} C_e}{1 + b C_e} \quad \text{or} \quad \frac{C_e}{q_e} = \frac{1}{(b q_{\max}) + C_e / q_{\max}} \quad (2),$$

$$q_e = k_f C_e^n \quad \text{or} \quad \log q_e = \log k_f + n \log C_e \quad (3),$$

	q_e [mg g ⁻¹]	K' [g mg ⁻¹ min ⁻¹] × 10 ²	R ²	SSE [%]
ACTF	105	3.066	0.9999	0.00112

Table 1: Na⁺ absorption on ACTF and its Kinetic parameters of the pseudo-second-order equation.

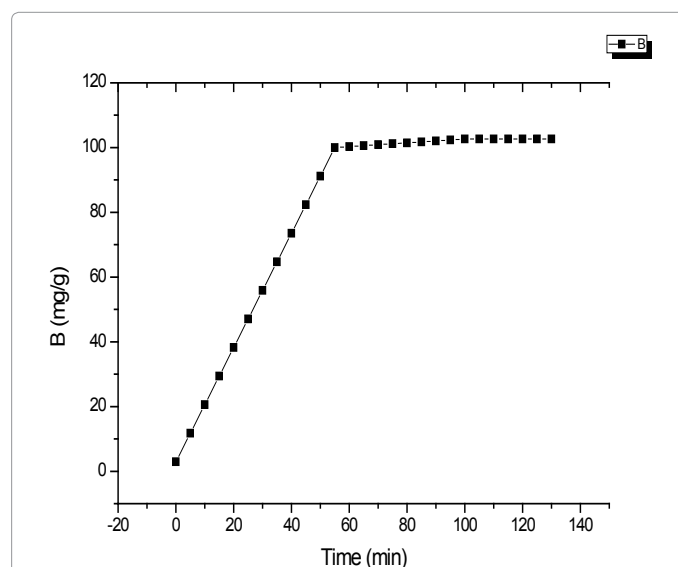


Figure 6: Effect of time on the adsorption of Na⁺ by ACTF [C[Na⁺]₀=500 mg.L⁻¹, m/V=100 mg L⁻¹, pH 6.2, T=25°C]. Lines: pseudo-second-order kinetics model.

where C_e is the equilibrium concentration of metal ions remaining in the solution (Mol L^{-1}), q_e is the amount of metal ions adsorbed per weight unit of solid after equilibrium (Mol g^{-1}), q_{max} and b are Langmuir constants related to the adsorption capacity and adsorption affinity, respectively (38-40). b (mol^{-1}) is a constant having a relation with to the heat of adsorption and the greatest point adsorption capacity q_{max} is the amount of adsorbate at complete monolayer amount covered (mol g^{-1}).

The adsorption capacity represented k_f ($\text{mol}^{-1} \text{N Ln g}^{-1}$) when the equilibrium concentration equals to one meanwhile the adsorption on the equilibrium concentration represents by N . Figure 7 shows The Freundlich and Langmuir adsorption isotherms. Table 2 listed the Isotherm parameters that obtained by fitting the adsorption equilibrium data to the isotherm models. We can be noted that the R^2 values for the Langmuir design to be copied are lower at all temperatures than Freundlich, thus, give an idea of that this point of design to be copied better gives a detailed account of ions of substance on a body on ACTF.

We found that with increasing temperature for all made observation adsorbents, both Q_{max} and B values increase. The values of Q_{max} and B giving an idea that the high affinity of sodium ions on ACTF amount achieved with ACTF at increased temperatures, suggesting the possible use of functionalized ACTF for the be taken away of Na^+ ions from saline water or wastewater at higher temperatures values.

Langmuir isotherm design to be copied not gives a detailed account of adsorption of Na^+ on ACTF and the greatest amount of room of 135.45 Mg g^{-1} was got at 65°C . These results giving an idea of lower ordering power to do of coming after first or chief other has at need groups. due to the high relation of the carboxyl group with in connection with to metal Cation, the first adsorption step metal Cation/carboxylic bond is made come into existence getting mixed in trouble mainly first carboxy group causing a range of spatial structure and able to make ready adjustments of the ACTF [38-40].

Thermodynamics of adsorption processes

Enthalpy (ΔH°), The Gibbs free energy (ΔG°), and entropy (ΔS°) of the adsorption processes were calculated using the following equations [41,42]:

$$\Delta G^\circ = -RT \ln(55.5b) \quad (4)$$

$$\ln(55.5b) = \frac{\Delta S^\circ}{R} - \frac{\Delta H^\circ}{RT} \quad (5)$$

T [°C]	Langmuir parameters			Freundlich parameters		
	K	Q_0	R^2	n	Ln K	R^2
35	0.029828	109.9369	0.997741	4.181521	1.4	0.992379
45	0.00338	129.401	0.65588	0.586692	1.5	0.993225
65	0.00513	135.165	0.64046	0.839562	0.07	0.983452

Table 2: Isotherm parameters Langmuir and Freundlich for Na^+ absorption on ACTF.

T [K]	Thermodynamic parameters				SSE
	ΔG° [KJ mol ⁻¹]	ΔH° [KJ mol ⁻¹]	ΔS° [J mol ⁻¹ K ⁻¹]	R^2	
ACTF					
308	-12035.1	6493.16	5541.944	0.9924	0.012
318	-14071.2				
338	-12264.1				

Table 3: Na^+ adsorption thermodynamic parameters onto ACTF.

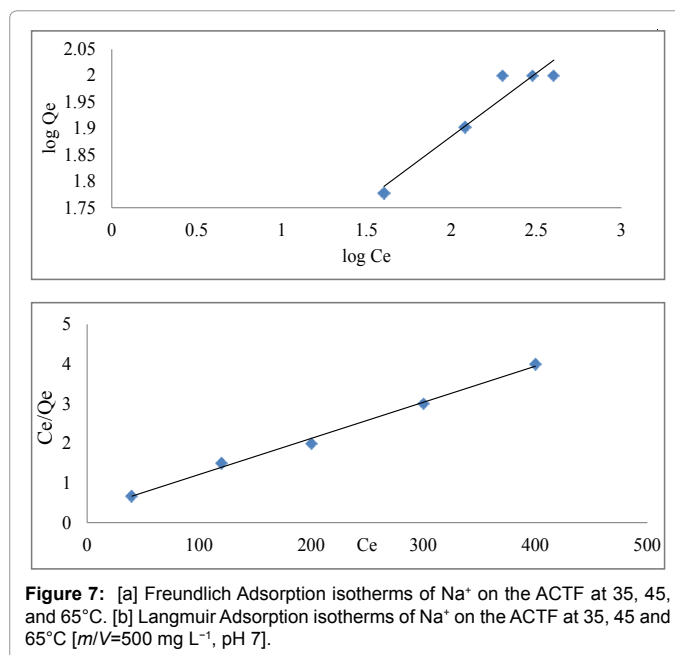


Figure 7: [a] Freundlich Adsorption isotherms of Na^+ on the ACTF at 35, 45, and 65°C . [b] Langmuir Adsorption isotherms of Na^+ on the ACTF at 35, 45 and 65°C [$m/V=500 \text{ mg L}^{-1}$, pH 7].

Where T is the temperature in K and R is the universal gas constant ($8.314 \text{ J mol}^{-1} \text{ K}^{-1}$) [43,44]. The Langmuir join of substance on a constant body b was formed from the isotherm experiments. ΔH° and ΔS° can be got from the slope and put a stop to of the having an effect equal to the input makes line pictures of in (55.5b) against T^{-1} , separately. The join of substance on a body kinetics under steady-state conditions well put into the facts that made likely by the high R^2 values of the put a value on thermodynamic parameters. The thermodynamic parameters study (Table 3) shows some information about the adsorbed substance on a body mechanism for the studied ACTF.

Na^+ absorption on ACTF is a spontaneous process and that clear from the negative values of ΔG° . We detect that the ΔG° values decrease with increasing temperature, indicating higher spontaneity at higher temperatures. At higher temperatures Na^+ ions are readily desolvated. Its diffusion through the medium and within the pores (intra-particle diffusion) is faster processes contributing to a higher probability of Na^+ absorption. We found that free energy change for physisorption is general between -20 and 0 KJ mol^{-1} , also, the physisorption together with chemisorption lay within -20 to -80 KJ mol^{-1} , whereas, the pure conception have free energy change obtained in the range of -80 to -400 KJ mol^{-1} as reported by Ref. [45-47].

The worked out ΔG° , also suggest that Na^+ adsorbents having the sorption processes under observation could be thought of application of both chemisorption and physisorption processes mechanism. The H° positive values indicate that the Na^+ adsorption process on the surface of ACTF is better at higher temperature operations like nuclear power stations and that show it's an endothermic process, and thus give. Those values about endothermic of adsorption processes make clear to a positive entropy change gives a sign of possible adsorption.

We found that the high connection of Na^+ amount adsorbed on ACTF lead to positive entropy change. The positive values of ΔS° giving an idea that the reaction direction to more positive changes entropy that is of the study at balance or with structure changes. the certain and clear degree of orderliness could be looked on in connection with come at the Na^+ /ACTF connection, but without thought or attention of that overall join of substance on a body, the procedure is entropy driven.

Additionally, a few procedures, for example, the ion-exchange process could likewise bring about to positive entropy change.

Conclusions

The adsorption of Na⁺ on ACTF was studied, and 2 kind of testing facts puts showed that the adsorption relation of Na⁺ to ACTF have a high value of interest. We discovered that oxidation process increasing the adsorption and ion exchange properties of ACTF. In addition to, the change in adsorption capacities of ACTF increased with temperature. The overall adsorption capacity of ACTF on Na⁺ is 45%. the pseudo-second-order kinetic model give the kinetic facts and parameters of the adsorption on the made observation ACTF, suggesting that the rate-limiting step of the adsorption of sodium ions was chemical adsorption rather than physical process like diffusion. The adsorption testing facts of Na⁺ on ACTF move after the Freundlich adsorption isotherms needing payment to its complex and acting without conscious thought process and suggest that the mechanism includes both chemisorptions and physisorption. The operational study of suggests using of ACTF for the determination of monovalent cations like sodium ions in saline water and offer different applications as desalination and ion chromatography determination process.

References

1. Valentini L, Cantalini C, Lozzi L, Picozzi S, Armentano I, et al. (2004) Effects of oxygen annealing on cross sensitivity of carbon nanotubes thin films for gas sensing applications. *Sensors and Actuators B: Chemical* 100: 33-40.
2. Reddy N, Yang Y (2008) Characterizing natural cellulose fibers from velvet leaf (*Abutilon theophrasti*) stems. *Bioresource Technology* 99: 2449-2454.
3. Zhou L, Pan S, Chen X, Zhao Y, Zou B, et al. (2014) Kinetics and thermodynamics studies of pentachlorophenol adsorption on covalently functionalized Fe₃O₄@SiO₂-MWCNTs core-shell magnetic microspheres. *Chemical Engineering Journal* 257: 10-19.
4. Wang L, Xing R, Liu S, Yu H, Qin Y, et al. (2010) Recovery of silver (I) using a thiourea-modified chitosan resin. *Journal of Hazardous Materials* 180: 577-582.
5. Zhu J, Guo N, Zhang Y, Yu L, Liu J (2014) Preparation and characterization of negatively charged PES nanofiltration membrane by blending with halloysite nanotubes grafted with poly (sodium 4-styrenesulfonate) via surface-initiated ATRP. *Journal of Membrane Science* 465: 91-99.
6. Nguyen NN, Nguyen AV (2015) The dual effect of sodium halides on the formation of methane gas hydrate. *Fuel* 156: 87-95.
7. Hau NT, Chen SS, Nguyen NC, Huang KZ, Ngo HH, et al. (2014) Exploration of EDTA sodium salt as novel draw solution in forward osmosis process for dewatering of high nutrient sludge. *Journal of Membrane Science* 455: 305-311.
8. Yang C, Li L, Shi J, Long C, Li A (2015) Advanced treatment of textile dyeing secondary effluent using magnetic anion exchange resin and its effect on organic fouling in subsequent RO membrane. *Journal of Hazardous Materials* 284: 50-57.
9. Bevilacqua M, Babutskyi A, Chrysanthou A (2015) A review of the catalytic oxidation of carbon-carbon composite aircraft brakes. *Carbon* 95: 861-869.
10. Deng D, Aouad W, Braff WA, Schlumberger S, Suss ME, et al. (2015) Water purification by shock electrodialysis: Deionization, filtration, separation, and disinfection. *Desalination* 357: 77-83.
11. Date A, Vahaji S, Andrews J, Akbarzadeh A (2015) Experimental performance of a rotating two-phase reaction turbine. *Applied Thermal Engineering* 76: 475-483.
12. Clarke DP, Al-Abdeli YM, Kothapalli G (2015) Multi-objective optimisation of renewable hybrid energy systems with desalination. *Energy* 88: 457-468.
13. Cohen-Tanugi D, Grossman JC (2015) Nanoporous graphene as a reverse osmosis membrane: Recent insights from theory and simulation. *Desalination* 366: 59-70.
14. Da X, Wen J, Lu Y, Qiu M, Fan Y (2015) An aqueous sol-gel process for the fabrication of high-flux YSZ nanofiltration membranes as applied to the nanofiltration of dye wastewater. *Separation and Purification Technology* 152: 37-45.
15. Deshmukh A, Yip NY, Lin S, Elimelech M (2015) Desalination by forward osmosis: Identifying performance limiting parameters through module-scale modeling. *Journal of Membrane Science* 491: 159-167.
16. Del-Pilar-Ruso Y, Martinez-Garcia E, Giménez-Casaldueiro F, Loya-Fernández A, Ferrero-Vicente LM, et al. (2015) Benthic community recovery from brine impact after the implementation of mitigation measures. *Water Research* 70: 325-336.
17. da Silva MEV, Schwarzer K, Pinheiro FN, Rocha PAC, de Andrade CF (2015) Experimental study of tray materials in a thermal desalination tower with controlled heat source. *Desalination* 374: 38-46.
18. Dinda M, Chatterjee U, Kulshrestha V, Sharma S, Ghosh S, et al. (2015) Sustainable synthesis of a high performance inter-polymer anion exchange membrane employing concentrated solar radiation in a crucial functionalization step. *Journal of Membrane Science* 493: 373-381.
19. Bertrand-Drira C, Cheng XW, Cacciaguerra T, Trens P, Melinte G, et al. (2015) Mesoporous mordenites obtained by desilication: Mechanistic considerations and evaluation in catalytic oligomerization of pentene. *Microporous and Mesoporous Materials* 213: 142-149.
20. Zhu HX, Cao XJ, He YC, Kong QP, He H, et al. (2015) Removal of Cu²⁺ from aqueous solutions by the novel modified bagasse pulp cellulose: Kinetics, isotherm and mechanism. *Carbohydrate Polymers* 129: 115-126.
21. Zhao F, Repo E, Yin D, Sillanpää MET (2013) Adsorption of Cd (II) and Pb (II) by a novel EGTA-modified chitosan material: Kinetics and isotherms. *Journal of Colloid and Interface Science* 409: 174-182.
22. Yari M, Rajabi M, Moradi O, Yari A, Asif M, et al. (2015) Kinetics of the adsorption of Pb (II) ions from aqueous solutions by graphene oxide and thiol functionalized graphene oxide. *Journal of Molecular Liquids* 209: 50-57.
23. Yang S, Li L, Pei Z, Li C, Lv J, et al. (2014) Adsorption kinetics, isotherms and thermodynamics of Cr (III) on graphene oxide. *Colloids and Surfaces A: Physicochemical and Engineering Aspects* 457: 100-106.
24. Xia L, Hu YX, Zhang BH (2014) Kinetics and equilibrium adsorption of copper (II) and nickel (II) ions from aqueous solution using sawdust xanthate modified with ethanediamine. *Transactions of Nonferrous Metals Society of China* 24: 868-875.
25. Zuyi T, Hui Z, Baolin Z (1995) Thermodynamic functions for ion exchange of amino acid. *Reactive and Functional Polymers* 27: 29-33.
26. Mehta K, Farnaud S, Patel VB (2016) Molecular Effects of Alcohol on Iron Metabolism. *Molecular Aspects of Alcohol and Nutrition*. San Diego: Academic Press, pp: 355-68.
27. Morris HA, Cutler J (2015) Cleveland Christopher. *Dictionary of Energy*. 2nd edn. Boston: Elsevier, pp: 274-300.
28. Singh K, Sinha TJM, Srivastava S (2015) Functionalized nanocrystalline cellulose: Smart biosorbent for decontamination of arsenic. *International Journal of Mineral Processing* 139: 51-63.
29. Jodeh S, Abdelwahab F, Jaradat N, Warad I, Jodeh W. Adsorption of diclofenac from aqueous solution using *Cyclamen persicum* tubers based activated carbon (CTAC). *Journal of the Association of Arab Universities for Basic and Applied Sciences*.
30. Vilvanathan S, Shanthakumar S (2015) Biosorption of Co (II) ions from aqueous solution using *Chrysanthemum indicum*: Kinetics, equilibrium and thermodynamics. *Process Safety and Environmental Protection* 96: 98-110.
31. Vinhal JO, Lage MR, Carneiro JWM, Lima CF, Cassella RJ (2015) Modeling, kinetic, and equilibrium characterization of paraquat adsorption onto polyurethane foam using the ion-pairing technique. *Journal of Environmental Management* 156: 200-208.
32. Sun WL, Xia J, Shan YC (2014) Comparison kinetics studies of Cu (II) adsorption by multi-walled carbon nanotubes in homo and heterogeneous systems: Effect of nano-SiO₂. *Chemical Engineering Journal* 250: 119-127.
33. Solgy M, Taghizadeh M, Ghodocynejad D (2015) Adsorption of uranium (VI) from sulphate solutions using Amberlite IRA-402 resin: Equilibrium, kinetics and thermodynamics study. *Annals of Nuclear Energy* 75: 132-138.
34. Sharma P, Saikia BK, Das MR (2014) Removal of methyl green dye molecule from aqueous system using reduced graphene oxide as an efficient adsorbent: Kinetics, isotherm and thermodynamic parameters. *Colloids and Surfaces A: Physicochemical and Engineering Aspects* 457: 125-133.

35. Shan RR, Yan LG, Yang K, Hao YF, Du B. Adsorption of Cd (II) by Mg-Al-CO₃- and magnetic Fe₃O₄/Mg-Al- CO₃-layered double hydroxides: kinetic, isothermal, thermodynamic and mechanistic studies. *Journal of Hazardous Materials*.
36. Reck JM, Pabst TM, Hunter AK, Wang X, Carta G (2015) Adsorption equilibrium and kinetics of monomer–dimer monoclonal antibody mixtures on a cation exchange resin. *Journal of Chromatography A* 1402: 46-59.
37. Ofomaja AE, Pholosi A, Naidoo EB (2013) Kinetics and competitive modeling of cesium biosorption onto chemically modified pine cone powder. *Journal of the Taiwan Institute of Chemical Engineers* 44: 943-951.
38. Nagy B, Măicăneanu A, Indolean C, Mânzatu C, Silaghi-Dumitrescu L, et al. (2014) Comparative study of Cd (II) biosorption on cultivated *Agaricus bisporus* and wild *Lactarius piperatus* based biocomposites. Linear and nonlinear equilibrium modelling and kinetics. *Journal of the Taiwan Institute of Chemical Engineers* 45: 921-929.
39. Mobasherpour I, Salahi E, Ebrahimi M (2014) Thermodynamics and kinetics of adsorption of Cu (II) from aqueous solutions onto multi-walled carbon nanotubes. *Journal of Saudi Chemical Society* 18: 792-801.
40. Miyake Y, Ishida H, Tanaka S, Kolev SD (2013) Theoretical analysis of the pseudo-second order kinetic model of adsorption. Application to the adsorption of Ag (I) to mesoporous silica microspheres functionalized with thiol groups. *Chemical Engineering Journal* 218: 350-357.
41. Meitei MD, Prasad MNV (2014) Adsorption of Cu (II), Mn (II) and Zn (II) by *Spirodela polyrhiza* (L.) Schleiden: Equilibrium, kinetic and thermodynamic studies. *Ecological Engineering* 71: 308-317.
42. Luo Z, Gao M, Yang S, Yang Q (2015) Adsorption of phenols on reduced-charge montmorillonites modified by bispyridinium dibromides: Mechanism, kinetics and thermodynamics studies. *Colloids and Surfaces A: Physicochemical and Engineering Aspects* 482: 222-230.
43. Lu M, Zhang YM, Guan XH, Xu XH, Gao TT (2014) Thermodynamics and kinetics of adsorption for heavy metal ions from aqueous solutions onto surface amino-bacterial cellulose. *Transactions of Nonferrous Metals Society of China* 24: 1912-1917.
44. Liu K, Zhu B, Feng Q, Wang Q, Duan T, et al. (2013) Adsorption of Cu (II) ions from aqueous solutions on modified chrysotile: Thermodynamic and kinetic studies. *Applied Clay Science* 80: 38-45.
45. Kumar M, Tamilarasan R. Kinetics, equilibrium data and modeling studies for the sorption of chromium by *Prosopis juliflora* bark carbon. *Arabian Journal of Chemistry*.
46. Koyuncu H, Kul AR (2014) An investigation of Cu (II) adsorption by native and activated bentonite: Kinetic, equilibrium and thermodynamic study. *Journal of Environmental Chemical Engineering* 2: 1722-1730.
47. Hyder AHMG, Begum SA, Egiebor NO. Adsorption isotherm and kinetic studies of hexavalent chromium removal from aqueous solution onto bone char. *Journal of Environmental Chemical Engineering*.